

Studies on the Low-Lying Levels of $\text{Ne}^{24}\dagger$

A. J. HOWARD,* R. G. HIRKO,‡ AND D. A. BROMLEY

Wright Nuclear Structure Laboratory, Yale University, New Haven, Connecticut 06520

AND

K. BETHGE§ AND J. W. OLNES

Brookhaven National Laboratory, Upton, New York 11973

(Received 19 November 1969)

Angular-distribution measurements have been performed on the $\text{Ne}^{22}(t, p)\text{Ne}^{24}$ reaction at $E_t=3.3$ MeV. Formation of the ground and 4.76-MeV Ne^{24} states is characterized by $l=0$ transfer, which establishes $J^\pi=0^+$ for these two states. The $J=2$, 3.87-MeV state was observed to be formed via $l=2$ transfer, and so even parity is indicated for this state. Proton- γ angular-correlation experiments were carried out in method II geometry at $E_t=3.45$ and 3.33 MeV. These results establish unambiguous $J=4$ and 2 assignments for the respective 3.96- and 5.58-MeV levels of Ne^{24} . The present experimental information on the static properties of Ne^{24} is shown to be consistent with a j - j coupling-model representation involving pure two-body proton configurations. An intercomparison of the observed static properties associated with the low-lying levels of the even- A neon isotopes is presented, and a remarkable similarity is shown to exist between the low-lying level structures of O^{18} and Ne^{24} . It is concluded that $1d_{5/2}$ subshell closure effects underlie the Ne^{24} spectrum.

I. INTRODUCTION

IN an extreme single-particle shell-model representation, the Ne^{24} nucleus consists of a closed $1d_{5/2}$ neutron subshell plus two protons, all external to the O^{16} nuclear structure. Considering isobaric spin, Ne^{24} is the $T_z=2$ member of the mass-24 system, for which the $T_z=0$ member is Mg^{24} . With the exception of the 0^+ , 15.43-MeV state, the $T=2$ members of Mg^{24} have not as yet been identified. The low-lying ($T=0$) levels of Mg^{24} , which is removed by an α particle from the doubly closed $1d_{5/2}$ subshell nucleus Si^{28} , possess both static and dynamic properties indicative of pronounced collective behavior. The degree to which the levels of the Ne^{24} isobar exhibit such behavior is of considerable importance as regards the T dependence of collective behavior within the $2s$ - $1d$ nuclear shell. In relation to this, it is of interest to examine the extent to which the properties of the Ne^{24} nucleus are similar to those previously established for O^{18} or for Ne^{18} , which are simply two identical nucleons external to O^{16} . Such a comparison can be interpreted as a measure of the degree to which $1d_{5/2}$ neutron subshell closure occurs in the Ne^{24} nuclear structure.

Experimentally, Ne^{24} is relatively inaccessible; the $\text{Ne}^{22}(t, p)\text{Ne}^{24}$ reaction ($Q_m=+5.60$ MeV) is the only conveniently employed route to this nucleus. Two such studies on the low-lying levels of Ne^{24} via the (t, p) reaction have been reported: (a) Silbert and Jarmie¹ have established the excitation energies E_x for eight

(and perhaps nine) states in Ne^{24} below $E_x=6.04$ MeV via magnetic-spectrograph studies at a fixed angle ($\theta_p=90^\circ$) with energy resolution of ± 20 keV; (b) Becker, Chase, McDonald, and Warburton² have further established both static and dynamic properties for the 1.99-, 3.87-, and 4.76-MeV Ne^{24} levels. This previously available information is summarized in Fig. 1.

The present work is primarily concerned with the four Ne^{24} states between $E_x=3.96$ and 5.58 MeV. Angular-distribution measurements were carried out on the protons from the $\text{Ne}^{22}(t, p)\text{Ne}^{24}$ reaction studied at $E_t=3.30$ MeV and are reported in Sec. II. Proton-gamma angular-correlation studies were performed on the $\text{Ne}^{22}(t, p\gamma)\text{Ne}^{24}$ reaction at $E_t=3.45$ and 3.33 MeV, and these experiments are presented in Sec. III. The implications associated with the known information on this $T_z=2$ member of the $A=24$ system are discussed in Sec. IV, in which a comparison is also made involving the known static properties of the low-lying levels of the even- A neon isotopes.

II. PROTON ANGULAR-DISTRIBUTION STUDIES ON THE $\text{Ne}^{22}(t, p)\text{Ne}^{24}$ REACTION

A 3.3-MeV triton beam from the 3.5-MV Brookhaven National Laboratory Van de Graaff accelerator was incident upon a Ne^{22} gas target of 95% isotopic and 99% elemental purities, which was confined at a pressure of 200 Torr in a 1-in.-diam cylindrical target cell mounted with its axis of revolution perpendicular to the beam vector and to the (horizontal) reaction plane. Incident tritons and emergent particles passed through an essentially continuous 0.1-mil Havar retaining window, which formed the cylindrical wall of the cell. Proton groups were energy-analyzed by a 700- μ

† Work partially supported under U.S. Atomic Energy Commission Contract No. AT(30-1)-3223.

* Permanent address: Trinity College, Hartford, Conn. 06106.

‡ Present address: Department of Physics, Stanford University, Stanford, Calif. 94305.

§ Summer visitor (1968) from the University of Pennsylvania, Philadelphia, Pa. Permanent address: Universität Heidelberg, Heidelberg, Germany.

¹ M. G. Silbert and N. Jarmie, Phys. Rev. **123**, 221 (1961).

² J. A. Becker, L. F. Chase, Jr., R. E. McDonald, and E. K. Warburton, Phys. Rev. **176**, 1310 (1968).

TABLE I. Optical-model parameters used in the DWBA analyses of the $\text{Ne}^{22}(t, p)\text{Ne}^{24}$ reaction, $E_t = 3.3$ MeV.

Particle	V_0 (MeV)	W (MeV)	r_0 (F)	a (F)	r_{0c} (F)	r_0' (F)	a' (F)	Ref.
Triton	140.0	30.0	1.28	0.65	1.30	1.28	0.65	5
Proton	60.0	8.2	1.25	0.65	1.25	1.25	0.68	6

solid-state detector, in front of which was placed a 2-mil-thick aluminum absorber foil in order to remove from the view of the detector scattered tritons and α particles from the $\text{Ne}^{22}(t, \alpha)\text{F}^{21}$ reaction. The use of this foil restricted the present investigation to Ne^{24} levels lying below $E_x = 5$ MeV. A two-aperture collimation system located before the detector was employed to define an interaction volume within the gas cell, and it also limited the angular divergence of detected protons to 1.5° . The proton-energy resolution obtained with this system was ~ 100 keV. Two such detection systems were constructed. One was used to measure

the proton angular distributions from $\theta_p = 10^\circ$ to 90° in the laboratory frame, while the other concurrently recorded monitor spectra at a fixed angle of -90° . Beam current was integrated in a Faraday cup located ~ 20 cm beyond the center of the gas cell. Because of significant uncertainties concerning the efficiency of beam collection in the scattering chamber containing the gas cell, it was judged that *absolute* differential cross sections were not reliably determinable in the present measurement. Thus, the monitor spectra described above were used as a normalization standard for determination of the *relative* differential cross sections as presented below.

Angular distributions were measured for the 0-, 1.99-, 3.87-, and 4.76-MeV Ne^{24} levels over the entire angular range studied and are presented in Fig. 2. The 3.96- and 4.89-MeV states were relatively weakly populated here, and no significant angular-distribution information was obtained concerning these two levels. As is evident in Fig. 2, the angular distributions associated with the formation of the ground, 3.87-, and 4.76-MeV states displayed definite direct-reaction characteristics. Distorted-wave Born-approximation (DWBA) analyses^{3,4} using the Oak Ridge computer program JULIE were applied to these data. The triton optical-model parameters used are those obtained by Glover and Jones,⁵ while the analogous proton parameters were taken from the review by Hodgson⁶; these are summarized in Table I. The DWBA fits generated are shown on solid curves in Fig. 2, where it is clear that both the ground and 4.76-MeV Ne^{24} angular distributions are well-fitted for an assumed $l=0$ transfer in their formation. Since $J^\pi = 0^+$ is certain for the Ne^{22} target nucleus, it follows that unique $J^\pi = 0^+$ assignments are indicated for both of these levels.

The 1.99- and 3.87-MeV Ne^{24} states have previously been indicated² to possess $J=2$, and it has also been previously shown² that the 1.99-MeV and ground levels probably possess like parity. The observed angular distribution for the 1.99-MeV state was essentially isotropic (see Fig. 2), and hence no direct evidence was

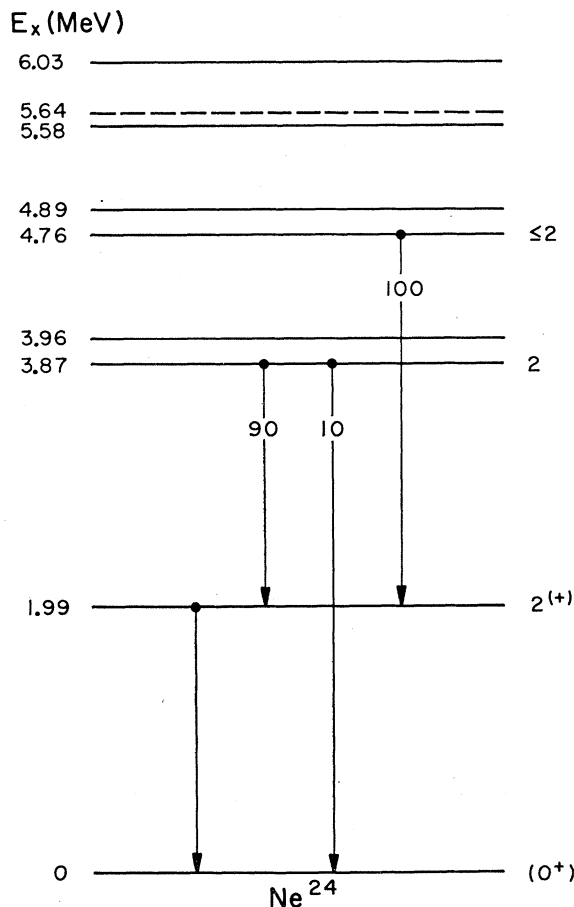


FIG. 1. Summary of previously reported experimental observations on the Ne^{24} nuclear structure. See Refs. 1 and 2 for details.

³ R. H. Bassel, R. M. Drisko, and G. R. Satchler, Oak Ridge National Laboratory Report No. ORNL-3240 (unpublished).

⁴ G. R. Satchler, Nucl. Phys. **55**, 1 (1964).

⁵ R. N. Glover and A. D. W. Jones, Nucl. Phys. **81**, 268 (1966).

⁶ P. E. Hodgson, *The Optical Model for Elastic Scattering* (Clarendon Press, Oxford, England, 1963).

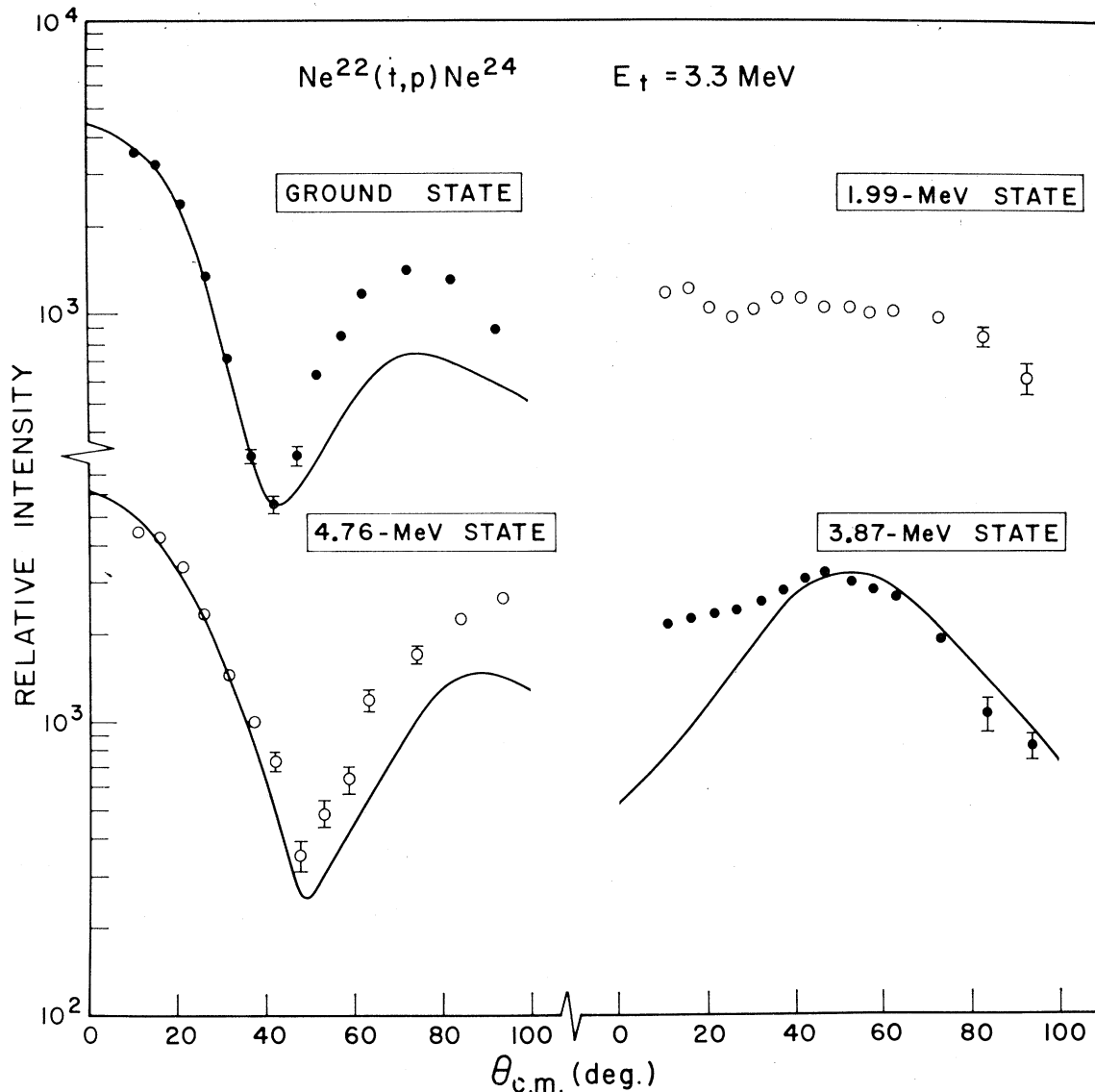


FIG. 2. Angular distributions of the proton groups from the $\text{Ne}^{22}(t, p)\text{Ne}^{24}$ reaction associated with formation of the ground, 1.99-, 3.87-, and 4.76-MeV states. The solid curves represent the DWBA fits discussed in the text: $l=0$ in the formation of the ground and 4.76-MeV states, and $l=2$ in the case of the 3.87-MeV state.

obtained on this state as regards its spin-parity in this investigation. The angular distribution associated with formation of the 3.87-MeV level is shown in Fig. 2 together with the DWBA fit generated for an assumed $l=2$ transfer. The poor fit to the extreme forward-angle data is here attributed to the employment of a single-nucleon form factor in the present analytical description of the reaction. An $l=2$ character for the transfer is nonetheless indicated by the fit to these data, and so the 3.87-MeV Ne^{24} state has positive parity.

We note that the previously reported conclusions of Becker *et al.*² on $p\text{-}\gamma$ correlation studies in the $\text{Ne}^{22}(t, p\gamma)\text{Ne}^{24}$ reaction contained the stated assumption that the Ne^{24} ground state has $J=0$. The present

results have determined rigorously $J^\pi=0^+$ for the ground state, and thus the assignments $J=2$ for both the 1.99- and 3.87-MeV states (as given in Fig. 1) are now also quite rigorous.

III. ANGULAR-CORRELATION STUDIES ON THE $\text{Ne}^{22}(t, p\gamma)\text{Ne}^{24}$ REACTION

The same gas-target material as described in Sec. II of this paper was employed for the present investigations. It was confined at a pressure of 250 Torr in a 0.6-cm-diam \times 0.6-cm-long cylindrical gas cell mounted with its axis of revolution colinear with the beam vector. Entrance and exit windows were made of 0.1-mil-thick

nickel foil. The cell was located in a previously described angular-correlation chamber.⁷ Protons that emanated from the reaction volume were observed by a 500- μ -thick annular detector, which was positioned at 4 cm from the target center so as to detect protons at $\theta_p \approx (170 \pm 3)^\circ$ from the beam axis. An appropriately placed aluminum foil, with either 1.50 or 1.25 mil thickness, removed scattered tritons and reaction α particles from the view of the particle detector. The observed energy resolution was ~ 100 keV.

Yield curves for the formation of states with $E_x \leq 6$ MeV in Ne^{24} were initially studied via direct spectra measured with the annular charged-particle detector. Measurements were made in 100-keV steps over the range of incident triton energies between $E_t = 2.50$ and 3.70 MeV. The results of this study indicated that the relative population of the 3.87- and 3.96-MeV Ne^{24} states, as observed at $\theta_p \sim 180^\circ$, changed markedly as a function of E_t . While the 3.87-/3.96-MeV-state population ratio was observed to be as large as $\sim 10:1$ at $E_t = 2.50$ MeV, this ratio was only 1:10 at $E_t = 3.45$ MeV. Hence the latter bombardment energy was selected as the most favorable energy for study of the 3.96-MeV state, since contamination from the 3.87-MeV state is minimal. These direct spectral studies also reveal that the 5.58-MeV state could be most effectively investigated at $E_t = 3.33$ MeV. Based on these considerations, method II angular-correlation measurements⁸ were subsequently performed at each of $E_t = 3.45$ and 3.33 MeV.

γ rays were detected in a 5-in.-diam \times 6-in.-long NaI(Tl) spectrometer, which was positioned with its front face 16 cm from the target center and was sequentially located (in random fashion) at $\theta_\gamma = 0^\circ, 30^\circ, 45^\circ, 60^\circ,$ and 90° with respect to the beam vector, with each angle repeated once. Time-coincident p - γ events were recorded in a two-parameter analysis with ~ 40 -nsec resolving time. A 128-channel (γ ray) by 128-channel (proton) data array was employed for these measurements. Analyses on 10 such data arrays essentially consisted of determining the γ -ray spectra which were time-coincident with selected regions of the proton spectra and were done with the aid of an IBM 7094 computer. Normalization of the γ -ray intensities so obtained from each data array was made according to the direct intensity of the 1.99-MeV-state proton group observed by the annular detector, which was concurrently recorded during the run at each angle θ_γ .

The proton spectrum observed in time coincidence with 1.99-MeV γ rays as measured for $E_t = 3.45$ MeV is illustrated in Fig. 3. Here, the total coincident proton spectrum demonstrates that the 3.87-/3.96-MeV-state population ratio was indeed ~ 0.1 , as was inferred from the direct-proton spectrum discussed earlier. The pres-

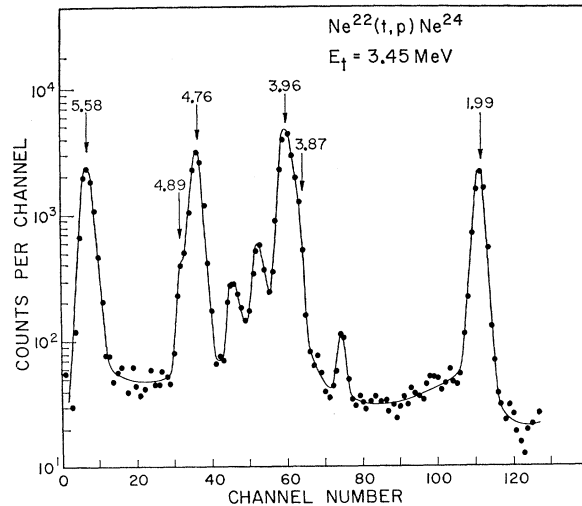


FIG. 3. Proton spectrum measured in time coincidence with 1.99-MeV γ rays. Proton groups identified with the $\text{Ne}^{22}(t, p)\text{Ne}^{24}$ reaction are labeled according to their excitation energies in Ne^{24} . The unlabeled peaks are associated with the $\text{Ne}^{20}(t, p)\text{Ne}^{22}$ reaction involving the 5% Ne^{20} isotopic content of the target.

ence of contaminant events, primarily associated with proton groups from the $\text{Ne}^{20}(t, p\gamma)\text{Ne}^{22}$ reaction involving the 5% Ne^{20} content of the target gas, is also evident in Fig. 3. However, angular-correlation studies were subsequently undertaken with a monoisotopic Ne^{20} target, and the results indicated that no ambiguities had been introduced into the present studies by this source of spectral contamination. A data array was also collected with the gas cell evacuated to 10^{-2} Torr so as to determine contributions from the cell windows; this result also indicated that no ambiguities were present because of this contamination source.

The extracted angular correlations thus determined were next fitted with the appropriate theoretical formalisms using a computer code described by Poletti and Warburton.⁹ Coefficients determined from an even-order Legendre polynomial fit to the correlation data are given in Table II. Method II geometry restricts the population of Ne^{24} substates relative to the beam axis to be of magnitude $|\alpha| = 0$ or 1, and deviations of the experimental particle geometry from colinearity were accounted for by admitting $\leq 10\%$ relative intensity of $|\alpha| = 2$ substates into the fitting procedure. The associated population parameters were employed as variables, and best fits were obtained to the experimental angular correlations for various assumed spin sequences and for discrete values of one multipole-amplitude ratio x . The goodness of fit obtained is expressed in the usual χ^2 representation, in which the expectation value for a correct solution is unity. In the following presentations, assumed spin sequences

⁷ A. R. Poletti, Phys. Rev. **153**, 1108 (1967).

⁸ A. E. Litherland and A. J. Ferguson, Can. J. Phys. **39**, 788 (1961).

⁹ A. R. Poletti and E. K. Warburton, Phys. Rev. **137**, B595 (1965).

TABLE II. Results of an even-order Legendre-polynomial fit of the form $W(\theta) = a_0 + a_2 P_2(\cos\theta) + a_4 P_4(\cos\theta)$ for $p\text{-}\gamma$ angular-correlation data in the $\text{Ne}^{22}(t, p\gamma)\text{Ne}^{24}$ reactions. Solutions for a_2 and a_4 and the normalized χ^2 are tabulated for the indicated transitions originating from deexcitation of the given initial states E_i . The normalization is such that $a_0 = 1$.

E_i (MeV)	Transition (MeV)	$a_2(\%)^a$	$a_4(\%)^a$	χ^2
1.99	1.99→0	+46.7±6.8	+18.4±8.3	1.06
3.96	3.96→1.99→0 ^b	+44.2±1.9	-35.8±2.5	0.35
4.76	4.76→1.99	-0.6±1.8	-0.6±2.3	0.59
	1.99→0	+3.4±2.7	-3.6±3.4	1.37
5.58	5.58→1.99	+53.6±6.4	-13.9±7.7	0.37
	1.99→0	+28.0±3.4	+47.9±4.3	1.75

^a The coefficients a_2 and a_4 have been corrected for the finite size of the γ -ray detector, using attenuation coefficients $Q_2 = 0.93$ and $Q_4 = 0.79$.

^b Correlation given is for net intensity of the unresolved members of this cascade.

for which the minimal χ^2 exceeds the 0.1% statistical-confidence limit were excluded from further consideration. For allowed spin sequences, the solutions for x were taken at the one-standard-deviation limit on χ^2 . Concomitant spin and multipole-amplitude-ratio limitations that resulted from the present studies are presented in the following subsections and are summarized in Table III.

A. 1.99-MeV State

It is immediately evident from the large $P_4(\cos\theta)$ dependence evident in the 1.99→0 correlation data (see Table II) that the 1.99-MeV level has $J \geq 2$. Since the Ne^{24} ground state has $J = 0$, as shown in Sec. II, the 1.99→0 transition is a pure multipole (i.e., $x \equiv 0$). Theoretical fits to the angular-correlation data (Table II) were attempted for assumed spins $J \leq 3$ for the 1.99-MeV level. The corresponding values of χ^2 , the normalized goodness-of-fit parameter, were 40 ($J = 0$), 6.5 ($J = 1$), 2.0 ($J = 2$), and 22 ($J = 3$). Thus, possibilities $J = 0, 1$, and 3 are excluded, as the minimum values of χ^2 exceed the 0.1% confidence limit, which corresponds to $\chi^2 = 5.4$ in the present studies. The χ^2 value for $J = 2$ is acceptable. We further note that the possibilities $J \geq 4$ have been excluded from the previously noted² restriction on the lifetime of this 1.99-MeV level,¹⁰ $\tau \leq 3 \times 10^{-8}$ sec, which would imply an unreasonable strength for a $L \geq 4$ transition deexciting the 1.99-MeV state. Thus, the present results confirm the $J = 2$ assignment for the 1.99-MeV level advanced previously.²

B. 3.96-MeV State

No information other than its existence in Ne^{24} has been previously reported concerning this level. The present results indicate that the major decay route for this level is the 3.96→1.99 transition. No evidence was

observed for the ground-state transition, an upper limit of $\leq 2\%$ being set for this possible decay route. While the two members of the 3.96→1.99→0 γ -ray cascade were unresolved in the NaI detector, the peak energy clearly corresponds to the deexcitation of the 3.96-MeV level, and not the nearby 3.87-MeV level. This latter level is known from the work of Becker *et al.*² to possess $J = 2$ and to deexcite via a 90% branch to the 1.99-MeV state and a 10% branch to the ground state. Hence, the possibility of spectral contamination from this source was further investigated by observing the behavior of the angular correlation as generated from the γ -ray spectra coincident with the individual proton channels that comprised the 3.96-MeV proton groups. This test indicated that the angular correlation illustrated in the upper portion of Fig. 4 and associated with the 3.96-MeV level was not significantly disturbed by the presence of the slight ($\leq 10\%$) 3.87-MeV state spectral contamination. In fitting this composite two-distribution correlation, possible $J = 0$ through 5 spin assignments were considered for the 3.96-MeV state,

TABLE III. Summary of available information on the $(L+1)/L$ multipole-mixing ratios for γ -ray transitions linking (as indicated) various states in Ne^{24} . Except as noted, the results are from the present work.

Transition (MeV)	J_i	J_f	$x, [(L+1)/L]$
1.99→0 ^a	2	0	$x \equiv 0$
3.87→1.99 ^b	2	2	$x = -(0.15 \pm 0.15)$ or $x = -(2.1 \pm 0.6)$
3.96→1.99	4	2	$x = +(0.07 \pm 0.05)$
4.76→1.99 ^a	0	2	$x \equiv 0$
5.58→1.99	2	2	$x = -(0.07 \pm 0.07)$

^a For these cases, where $L = J_i - J_f$ and thus $x \equiv 0$, the present results are in agreement with the previous results of Ref. 2, thus confirming the conclusions on allowed values of J_i .

^b From Ref. 2.

¹⁰ D. H. Wilkinson, in *Nuclear Spectroscopy*, edited by F. Ajzenberg-Selove (Academic Press Inc., New York, 1960), Part B, p. 852 ff.

and $x=0$ was again employed for the $2^+, 1.99 \rightarrow 0^+, 0$ transition. As indicated in the lower portion of Fig. 4, a $J=4$ assignment for the 3.96-MeV level is uniquely indicated by this analysis. The value $x = +(0.07 \pm 0.05)$ here indicated for the $3.96 \rightarrow 1.99$ transition may very well reflect the presence of γ rays with $\sim 10\%$ relative intensity that originate from the $J=2, 3.87$ -MeV level, as discussed above. Such contamination would be consistent with a shift of the minimum in χ^2 from $x=0$ (i.e., pure-quadrupole radiation) to $x = +(0.07 \pm 0.05)$, as depicted in Fig. 4. Note that no further substantive alterations occur (due to the $3.87 \rightarrow 1.99 \rightarrow 0$ Ne^{24} intensity) as regards the results presented in Fig. 4. In

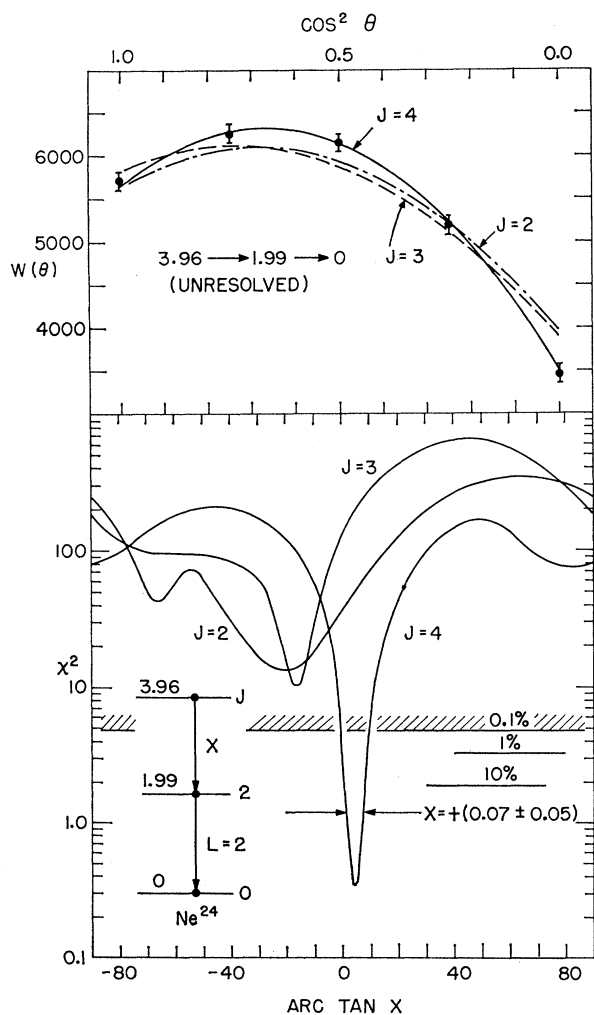


FIG. 4. Summary of the angular-correlation information concerning the 3.96-MeV state. The upper portion of the figure displays the experimental correlation data for the unresolved members of the $3.96 \rightarrow 1.99 \rightarrow 0$ cascade. The lower portion illustrates χ^2 as a function of $\arctan x$ for simultaneous fits to the unresolved $3.96 \rightarrow 1.99$ and $1.99 \rightarrow 0$ distributions under the assumptions presented in the inset energy-level diagram. Also shown in the upper portion are the best fits for $J=2, 3$, and 4 assignments for the 3.96-MeV level.

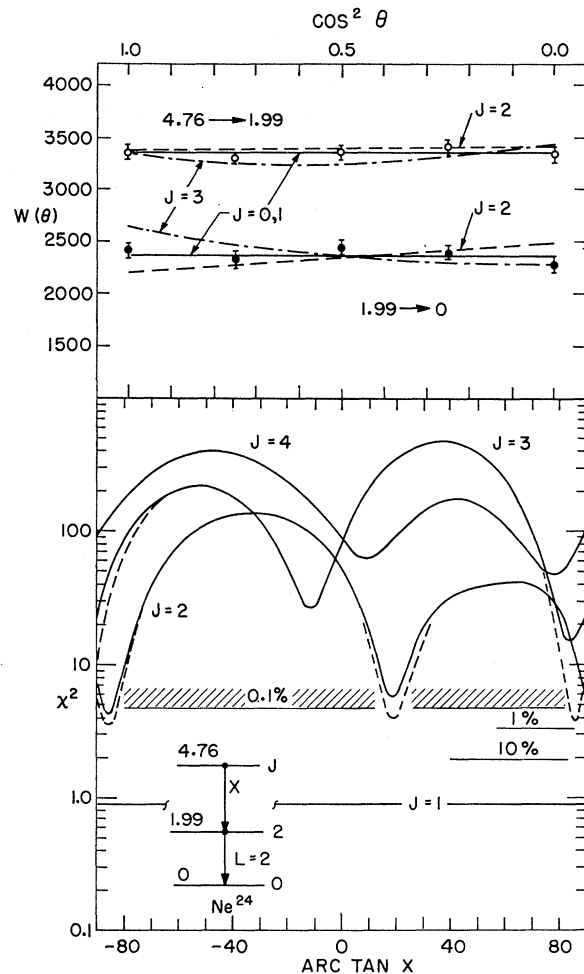


FIG. 5. Summary of angular-correlation information concerning the 4.76-MeV state. The $4.76 \rightarrow 1.99$ and $1.99 \rightarrow 0$ distributions are shown in the upper portion of the figure. χ^2 versus $\arctan x$ is illustrated in the lower portion for simultaneous fits to these two distributions. The dashed curve represents the fit obtained by including the finite-size effect in the fitting procedure. Not illustrated is $\chi^2=0.9$ for $J=0, x=0$.

summary, the $J=4$ assignment is unique and independent of this possible contamination source.

C. 4.76-MeV State

A $J^\pi=0^+$ assignment has been established for this level in Sec. II of this paper. As in the results of a previous study,² the only discerned decay route involves the $4.76 \rightarrow 1.99 \rightarrow 0$ cascade. The upper portion of Fig. 5 demonstrates that these two γ -ray distributions both appeared isotropic, consistent with the $J=0$ assignment made in Sec. II for the 4.76-MeV state. The results of Becker *et al.*² have indicated $J=0, 1$ for this level, with $J=2$ ruled against at the 5% confidence limit. When incorporated with the present results, $J=2$ is ruled against at the 0.1% limit and is thus excluded. In summary, p - γ angular-correlation data

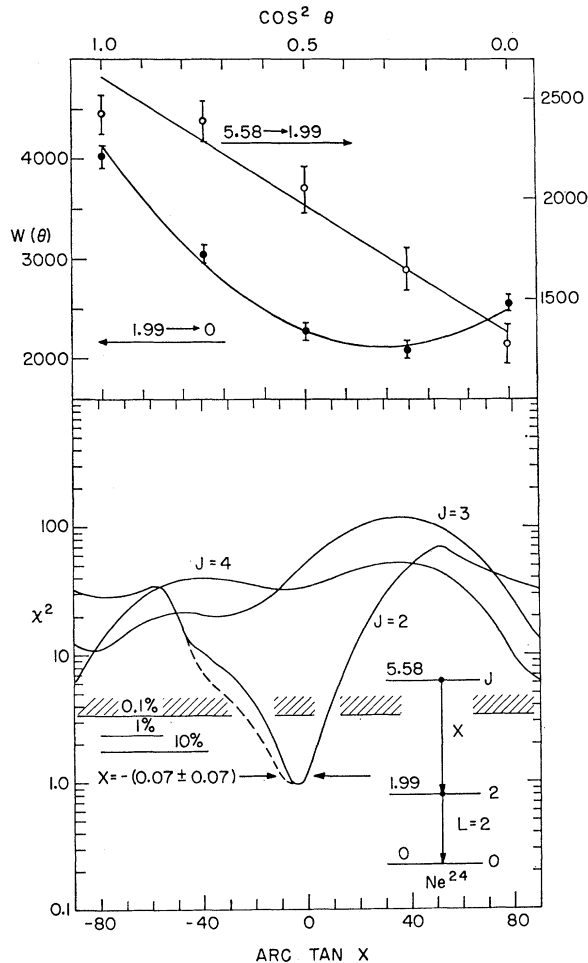


FIG. 6. Summary of angular-correlation information concerning the 5.58-MeV state. The $5.58 \rightarrow 1.99$ and $1.99 \rightarrow 0$ distributions are shown in the upper portion of the figure. χ^2 versus $\arctan x$ is illustrated in the lower portion for simultaneous fits to these two distributions. The dashed curve represents the fit obtained by including the finite-size effect in the fitting procedure.

determine $J=0, 1$ for the 4.76-MeV Ne^{24} level, which is consistent with the $J^\pi=0^+$ assignment made in Sec. II.

D. 4.89-MeV State

No information has previously been reported concerning the properties associated with this level. It was relatively weakly populated in the present studies, and it was possible only to determine that the major decay route for this state is via a transition to the 2^+ , 1.99-MeV state.

E. 5.58-MeV State

The study of Silbert and Jarmie¹ established the definite existence of a state at $E_x=5.58$ MeV in Ne^{24} . Similar evidence concerning a possible state at $E_x=5.64$ MeV is considerably less certain. Internal calibrations of the γ -ray energy observed for the transition(s) from

these states to the 1.99-MeV state as measured in coincidence with the relevant proton group(s) indicated that the observed angular correlations involve only the 5.58-MeV, and not the 5.64-MeV, state. Furthermore, the possible influence on the results presented in Fig. 6 because of contributions from the possible 5.64-MeV state were found to be negligible via the same type of test as applied to the analyses of the 3.96-MeV Ne^{24} data presented in Sec. III B. The only discerned decay route involved the $5.58 \rightarrow 1.99 \rightarrow 0$ cascade, other branches being $<5\%$ in relative intensity. The two-distribution fit establishes $J=2$ for the 5.58-MeV level and also indicates a predominant dipole character, i.e., $x = -(0.07 \pm 0.07)$, for the $5.58 \rightarrow 1.99$ transition.

F. Lifetime Information on Ne^{24} States

From a comparison of the intensity of the individual proton peaks measured in coincidence with the corresponding deexcitation γ rays and the corresponding peaks as viewed in the proton-singles spectra, an upper limit of $\tau \leq 3 \times 10^{-8}$ sec is placed on the lifetimes of the initial γ -ray emitting states as determined from the resolving time ($2\tau=40$ nsec) of the p - γ coincidence circuit. This information has been used in the above considerations to independently rule out spin assignments that would involve deexcitation γ rays of $L \geq 4$ since the strengths of such transitions would be prohibitively large, i.e., $|M|^2 > 7000$.¹⁰

It is also noted that the principal deexcitation of the 1.99-, 3.96-, and 4.76-MeV Ne^{24} states occurs via emission of $L=2$ radiation to lower-lying states. The lifetimes of these initial states are therefore probably in the range accessible to measurement by the Doppler-shift attenuation method (DSAM),¹¹ provided one uses a solid stopping medium for the recoil Ne^{24} ions. Both the present and previous² experiments discussed in this paper have utilized Ne^{22} gas for the target and stopping media. In this case, the characteristic stopping time ($\alpha \sim 300$ psec) would be too long to permit meaningful lifetime measurements for these states via the DSAM method.

For a solid target, however, the results could in principle distinguish between $E2$ and $M2$ radiations. Such an experiment has recently been performed using the DSAM method to measure Ne^{24} lifetimes for states formed from Ne^{22} bombardment of a solid-tritium target.¹² The results indicate $\tau = (1.0_{-0.4}^{+0.2})$ psec for the 1.99-MeV level, and $\tau < 100$ psec for the 3.87-MeV level. These lifetime results indicate that the $1.99 \rightarrow 0$ transition is $E2$, rather than $M2$, and thus the 1.99-MeV level has the same parity as the ground state, which in the present experiment has been established as even

¹¹ A. Z. Schwarzschild and E. K. Warburton, Ann. Rev. Nucl. Sci. **18**, 265 (1968).

¹² K. Bharuth-Ram, K. P. Jackson, K. W. Jones, and E. K. Warburton, Nucl. Phys. **A137**, 262 (1969).

(Sec. II). Similarly, a strong preference is exhibited for an $E2$ character in the $3.87 \rightarrow 1.99$ transition, thus supporting the conclusions reported above in Sec. II.

IV. DISCUSSION

With regard to static properties, rigorous spin assignments as summarized in Secs. II and III are now available for six of the eight lowest-lying levels of Ne^{24} . Positive parity is established for the ground, 3.87-, and 4.76-MeV states as a result of the proton angular-distribution measurements reported in Sec. II. Positive parity is also favored from general considerations based on systematic behavior in this mass region for both the $J=2$, 1.99-MeV and $J=4$, 3.96-MeV Ne^{24} levels. It is thus probable that the five lowest-lying levels of Ne^{24} are of positive parity, and this is assumed in the following presentation. The observed static properties of Ne^{24} are summarized in Fig. 7, in which similar information¹³⁻¹⁹ on the even-neutron count $N=8$, 10, and 12 neon isotopes is also presented for states below an excitation energy of 6 MeV. The O^{18} structure given in Fig. 7 represents the net information on the O^{18} - Ne^{18} mirror-pair system. From an intercomparison of the information concerning these four isotopes, several observations support the postulate that the Ne^{24} spectrum displays behavior characteristic of the effects of $1d_{5/2}$ neutron-shell closure.

It is evident in Fig. 7 that a marked similarity exists between the low-lying positive-parity structure of O^{18} and Ne^{24} . Concerning detailed description of the observed properties associated with normal-parity states of the O^{18} - Ne^{18} mirror-pair system, it has been previously demonstrated²⁰ that the inclusion of modest collective behavior is not only effective, but also probably mandatory. The fact remains that the gross features observed for the mass-18 mirror pair are accounted for by a j - j coupling shell-model approach^{21,22} involving $1d_{5/2}$ and $2s_{1/2}$ orbits for the two neutrons beyond O^{16} . It follows that Ne^{24} may be equivalently well-represented by this approach with two protons beyond a double-

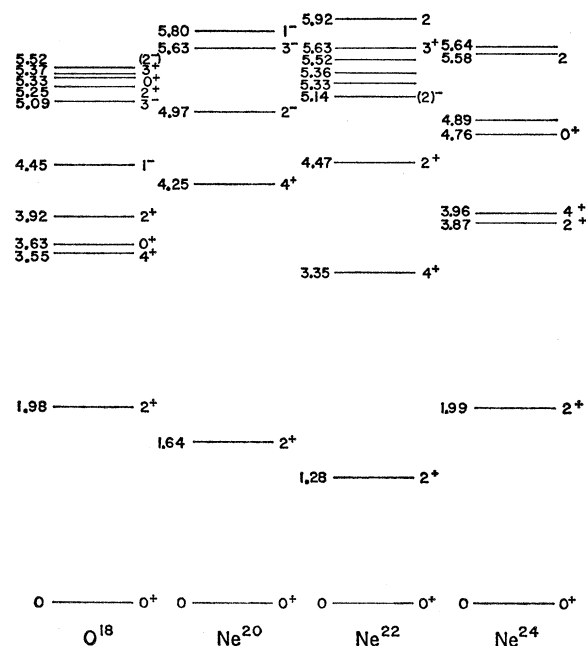


Fig. 7. Summary of the static properties observed for levels of O^{18} , Ne^{20} , Ne^{22} , and Ne^{24} below 6-MeV excitation energy. The data presented is taken from the following sources: O^{18} , Refs. 13 and 14; Ne^{20} , Ref. 15; Ne^{22} , Refs. 16-19; Ne^{24} , Refs. 1, 2, and the present work.

closed-core structure. Thus the ground, 1.99-, and 3.96-MeV Ne^{24} levels may be viewed as the respective 0^+ , 2^+ , and 4^+ states based on essentially pure $(1d_{5/2})^2$ proton configurations. In similar fashion, the 2^+ , 3.87-MeV and 0^+ , 4.76-MeV levels are represented as pure $(1d_{5/2})(2s_{1/2})$ and $(2s_{1/2})^2$ configurations, respectively. The shell-model predictions generated by Talmi and Unna²¹ as to the location of these model states are found to be in remarkably good agreement with their observed counterparts in Ne^{24} .

When the Ne^{20} and Ne^{22} structures are brought into consideration, it becomes apparent that several pronounced differences exist between the low-lying level locations in these two neon isotopes and the two just discussed. The spacings of the lowest-lying 0^+ , 2^+ , and 4^+ levels in Ne^{20} and Ne^{22} approach the $J(J+1)$ dependence characteristic of pronounced rotational behavior (this dependence is further supported by the observed positions of the relevant 6^+ , 8^+ Ne^{20} and 6^+ Ne^{22} states). This is in contrast to the simple J -dependent harmonic-oscillator location associated with these states in O^{18} and Ne^{24} . The location of the second 0^+ state in each of the four nuclei under discussion also supports the contention that the Ne^{24} spectrum displays a reversion towards that of O^{18} . Experimentally, $E_x=3.63$, 6.71, 6.24, and 4.76 MeV for the second 0^+ level in O^{18} , Ne^{20} , Ne^{22} , and Ne^{24} , respectively. A similar situation is discerned in the locations of the second 2^+ member in these systems: $E_x=3.92$, 7.43, 4.47, and 3.87 MeV, respectively. It is thus indicated that addi-

¹³ R. W. Ollerhead, J. S. Lopes, A. R. Poletti, M. F. Thomas, and E. K. Warburton, Nucl. Phys. **66**, 161 (1965).

¹⁴ J. S. Lopes, O. Hausser, R. D. Gill, and H. J. Rose, Nucl. Phys. **89**, 127 (1966).

¹⁵ T. Lauritsen and F. Ajzenberg-Selove, in *Nuclear Data Sheets*, compiled by K. Way *et al.* (Printing and Publishing Office, National Academy of Sciences—National Research Council, Washington 25, D.C., 1962).

¹⁶ S. Buhl, D. Pelte, and B. Povh, Nucl. Phys. **A91**, 319 (1967) and references therein.

¹⁷ W. Kutschera, D. Pelte, and G. Schrieder, Nucl. Phys. **A111**, 529 (1968).

¹⁸ W. Scholz, P. Neogy, K. Bethge, and R. Middleton, Phys. Rev. Letters **22**, 949 (1969).

¹⁹ A. J. Howard, J. G. Pronko, and R. G. Hirko (to be published).

²⁰ H. G. Benson and J. M. Irvine, Proc. Phys. Soc. (London) **89**, 249 (1966).

²¹ I. Talmi and I. Unna, Nucl. Phys. **30**, 280 (1962).

²² A. Arima, S. Cohen, R. D. Lawson, and M. H. Macfarlane, Nucl. Phys. **A108**, 94 (1968).

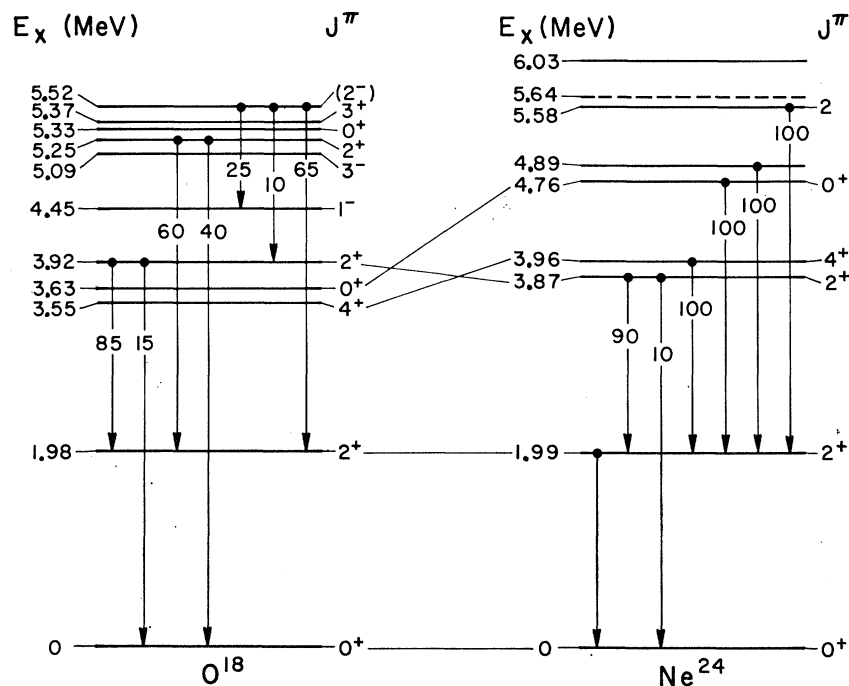


FIG. 8. Intercomparison of properties associated with the O^{18} and Ne^{24} nuclear structures. Selected branching-ratio information for O^{18} as discussed in the text is shown; see Refs. 13 and 14 for details.

tion of a $1d_{5/2}$ neutron pair to Ne^{18} creates a strong perturbation on the initial system, as is manifested by the Ne^{20} level structure for which a pure $j-j$ coupling representation is grossly inadequate. Addition of another neutron pair to form Ne^{22} results in a spectrum suggestive of continued perturbation. The addition of the final neutron pair to form Ne^{24} results in a spectrum indicative of subshell closure and is described to first order by the aforementioned two-body pure $j-j$ coupling representation.¹⁸ A symmetry centered about $A=21$ exists concerning the level sequences depicted in Fig. 7. This behavior appears to be directly correlated with the degree of completeness of the $1d_{5/2}$ neutron subshell. The number N of $1d_{5/2}$ neutron particles (or holes, whichever is less) equals 0 for Ne^{18} and Ne^{24} and equals 2 for Ne^{20} and Ne^{22} . This observation is consistent with the situation for the odd- A neon isotopes: The Ne^{21} nuclear structure, for which $N=N_{max}=3$, is perhaps the most strongly deformed nucleus in the $2s-1d$ shell; in contrast, Ne^{19} and Ne^{23} ($N=1$) display less-marked collective effects. It should be noted that this systematic examination of these neon isotopes supports a subshell-closure argument as underlying the Ne^{24} spectrum rather than a destruction of collectivity through the augmented neutron pairing permitted by the increased T of this nucleus. The latter argument, although certainly retaining some validity, could not result in the apparent similarities between the mass-18 and mass-24 neon isotopic structures.

The degree to which the O^{18} and Ne^{24} nuclear structures are equivalent has emerged as a question of high

interest, and so the observed dynamic properties associated with these two nuclei are also compared. There is a general lack of information concerning absolute electromagnetic-transition rates in Ne^{24} , but delimitations of branching and/or multipole-amplitude ratios have been made for most of these states. Branching-ratio information associated with Ne^{24} levels as well as the $J=2$ levels in O^{18} is presented in Fig. 8. Of primary interest here are the γ -ray deexcitation properties associated with the 3.87- and 5.58-MeV Ne^{24} states and candidates for their assumed equivalent levels in O^{18} . The dynamic properties associated with the 2^+ , 3.87-MeV Ne^{24} state indicate^{2,12} that the $M1$ component dominates the 90% branch to the 1.99-MeV level ($x=-0.15\pm 0.15$), and it therefore follows that the second 2^+ level in this nucleus is not vibrational in character. This situation is closely analogous to that associated with the 2^+ , 3.92-MeV O^{18} state, for which the dipole/quadrupole mixing is $x=+0.18\pm 0.10$ for the 85% branch to the 1.98-MeV state.¹³ Hence, an equivalency of the second 2^+ levels in these nuclear structures is supported by their observed dynamic behavior. The $J=2$, 5.58-MeV Ne^{24} state has been found to decay by a $>95\%$ branch to the 1.99-MeV state via a predominantly dipole transition ($x=-0.07\pm 0.07$). Two equivalent structure candidates exist in O^{18} , namely, the 2^+ , 5.25-MeV and (2^-) , 5.52-MeV states. As is apparent in Fig. 8, substantial alternate decay routes exist in addition to the predominant transition to the 1.98-MeV level for both of these states. This intercomparison does not determine which of these two O^{18}

levels is the more probable 5.58-MeV counterpart but does indicate the first substantial difference observed among the properties of the O¹⁸ and Ne²⁴ nuclear structures.

In summary, it has been demonstrated that the low-lying levels of the Ne²⁴ nuclear structure possess properties that are generally compatible with a simple two-body j - j -coupling shell-model representation involving essentially pure configurations. It thus appears that the effects of $1d_{5/2}$ subshell closure are important in the description of nuclei in this mass region, in which

the existence of pronounced collective behavior has been previously well documented.

ACKNOWLEDGMENTS

The Yale authors wish to express their appreciation to Dr. D. E. Alburger for the hospitality extended to them at Brookhaven during the course of these measurements. Discussions with Dr. J. A. Becker concerning previous work on Ne²⁴ are gratefully acknowledged. We also thank Dr. W. W. Watson for supplying the gas-target material used in these studies.

Study of the (d, t) Reaction on Si²⁸, S³², and Ar³⁶†

C. A. WHITTEN, JR.,* M. C. MERMAZ,† AND D. A. BROMLEY

Wright Nuclear Structure Laboratory, Yale University, New Haven, Connecticut 06520

(Received 19 November 1969)

The Si²⁸ (d, t) Si²⁷ reaction and the S³² (d, t) S³¹ and Ar³⁶ (d, t) Ar³⁵ reactions were studied at deuteron energies of 21.6 and 21.0 MeV, respectively. Angular distributions were obtained for triton groups from these (d, t) reactions leading to levels in the residual nuclei Si²⁷, S³¹, and Ar³⁵ with excitation energies up to approximately 3.5 MeV. Spectroscopic factors for the strong (d, t) transitions were extracted using now standard distorted-wave Born-approximation (DWBA) analyses. The (d, t) spectroscopic factors from this work are in reasonable agreement with previous neutron-pickup experimental data on Si²⁸, S³², and Ar³⁶, whenever the latter are available. Recent $2s$ - $1d$ shell-model calculations are in reasonable accord with these data. In the particular case of the Ar³⁶ (d, t) Ar³⁵ data, it appears that the theoretical calculation which uses a "realistic" interaction derived from nucleon-nucleon scattering gives better agreement with these data than the theoretical calculation which uses a modified surface δ interaction.

I. INTRODUCTION

THIS paper represents the second in a series of three papers dealing with deuteron induced reactions on the even-even, $T=0$, target nuclei Si²⁸, S³², and Ar³⁶, which lie in the upper half of the s - d shell. The first paper¹ in this series presented data for the (d, d) and (d, d') reactions on the above mentioned nuclei, while the present work and the third paper² present data for the (d, t) and (d, p) reactions, respectively. The general purpose of this series of experiments has been to investigate the equilibrium shape of these nuclei using the (d, d') reaction and also to investigate the neutron hole and neutron particle structure relative to these even-even cores with the (d, t) and (d, p) reactions, respectively. In the case of Si²⁸ it had been sug-

gested³ that the combination of single nucleon pickup and stripping reactions on this target nucleus could be used to study possible changes in the equilibrium shape of the core as a nucleon is either added to or subtracted from that core.

Considerable data have been reported for the single neutron pickup reactions (p, d) ⁴⁻⁶ and (He^3, α) ⁷⁻⁹ on Si²⁸, S³², and Ar³⁶; the present work, however, represents the first study of the (d, t) reaction on these target nuclei. The very large neutron binding energies for these even-even, $T=0$, target nuclei—ranging from 15.09 MeV in S³² to 17.18 MeV in Si²⁸—made it necessary to use incident deuteron energies of ~ 21 MeV in order to study a reasonable range of excitation

† Work supported in part by the U.S. Atomic Energy Commission under Contract No. AT(30-1)3223.

* Present address: Department of Physics, University of California, Los Angeles, Calif. 90024.

† NATO Fellow on leave of absence from the Center of Nuclear Research, Saclay, France. Present address: Center of Nuclear Research, Saclay, France.

¹M. C. Mermaz, C. A. Whitten, Jr., and D. A. Bromley, Phys. Rev. **187**, 1466 (1969).

²M. C. Mermaz, C. A. Whitten, Jr., J. W. Champlin, A. J. Howard, and D. A. Bromley (to be published).

³G. Ripka, in *Proceedings of the International Nuclear Physics Conference, Gallinburg, Tennessee, 1966* (Academic Press, Inc., New York, 1967), p. 833.

⁴G. D. Jones, R. R. Johnson, and R. J. Griffiths, Nucl. Phys. **A107**, 659 (1968).

⁵R. R. Johnson and R. J. Griffiths, Nucl. Phys. **A108**, 113 (1968).

⁶R. L. Kozub, Phys. Rev. **172**, 1078 (1968).

⁷B. H. Wildenthal and P. W. M. Glaudemans, Nucl. Phys. **A92**, 353 (1967).

⁸L. W. Swenson, R. W. Zurmühle, and C. M. Fou, Nucl. Phys. **A90**, 232 (1967).

⁹C. M. Fou and R. W. Zurmühle, Phys. Rev. **151**, 927 (1966).